Talisman 4.0

A finite volume–finite element tool for numerical simulation of subsurface flow and contaminant transport with a posteriori error control and adaptive mesh refinement

Technical documentation

Martin Vohralík[1]

February 28, 2007

[1] Laboratoire Jacques-Louis Lions
Université Pierre et Marie Curie (Paris 6)
175 rue du Chevaleret, 75 013 Paris, France
vohralik@ann.jussieu.fr

Contents

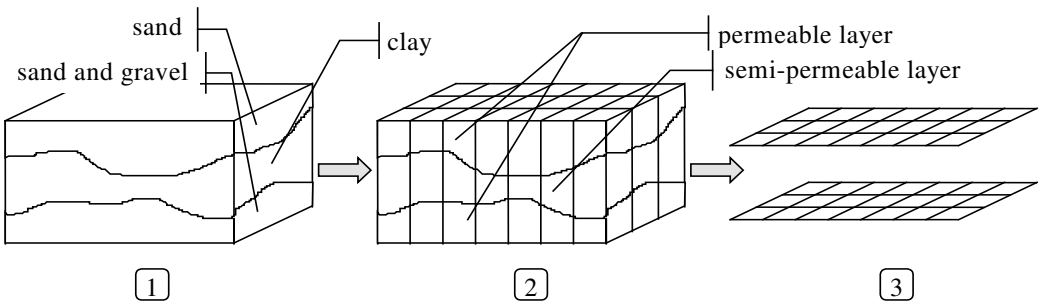

Figure 1: A typical layered subsurface

1 Purpose of this manual

The purpose of this manual is to give a technical documentation to the Talisman code. As such, it complements the Presentation and User guide [15] and the Developer's manual [14]. In particular, the description of admissible geometries, detailed form of the equations simulated in Talisman, description of numerical schemes implemented in Talisman, of the nonlinear and linear solvers, and a detailed form of the error estimates and adaptive refinement algorithms implemented in Talisman is given here and in the cited references.

2 Domain and equations

We describe here in detail the domain and equations considered in Talisman.

2.1 Types of domain

A typical porous media is composed of several superposing geological layers, cf. Figure 1. Three types of representation of these domain exist under Talisman.

- **3D** The entire subsurface domain is represented, which corresponds to the left part of Figure 1.
- **2D multi-layer** Only the permeable aquifers are represented, which is indicated in the right part of Figure 1.
- **2D** A vertical cut of the three-dimensional domain is considered, so that the final domain is two-dimensional.

2.2 Flow equation

Three types of equations, corresponding to the chosen subsurface representation, are at disposition in Talisman.

2.2.1 Richards equation

Richards equation is recognized for describing accurately enough two-phase water–air flow in the subsurface, see e.g. [1, 3, 8, 16]. Let $(0,T)$ be a time interval, $0 < T < +\infty$, and let Ω correspond to the entire subsurface domain (3D case) or possibly to the 2D cut, and let $\overline{\Gamma_{\rm D}} \cup \overline{\Gamma_{\rm N}} = \partial\Omega$, $\Gamma_{\rm D} \cap \Gamma_{\rm N} = \emptyset$, $|\Gamma_{\rm D}| \neq 0$, where $|\Gamma_{\rm D}|$ is the measure of the set $\Gamma_{\rm D}$. We write the Richards equation under the form

$$\begin{aligned}
\frac{\partial\theta(\psi)}{\partial t} - \nabla\cdot\mathbf{K}(\psi)\nabla(\psi+z) &= q_{\rm out}+q_{\rm in} \quad \text{in } \Omega\times(0,T)\,, && (2.1a)\\
\psi(\cdot,0) &= \psi_0 \quad \text{in } \Omega\,, && (2.1b)\\
\psi &= \psi_D \quad \text{on } \Gamma_{\rm D}\times(0,T)\,, && (2.1c)\\
-\mathbf{K}(\psi)\nabla(\psi+z)\cdot\mathbf{n} &= u_N \quad \text{on } \Gamma_{\rm N}\times(0,T)\,. && (2.1d)
\end{aligned}$$

Here, $\psi = \psi(\mathbf{x},t)$ is the pressure head ([L]), $\psi = p/\rho g$, where p ($[\mathrm{ML}^{-(d-2)}\mathrm{T}^{-2}]$) is the water pressure, ρ ($[\mathrm{ML}^{-d}]$) is the water density, and g ($[\mathrm{LT}^{-2}]$) is the gravitational acceleration constant, $z = z(\mathbf{x})$ is the elevation, the upward vertical coordinate ([L]), $\theta = \theta(\mathbf{x},\psi)$ is the water content ([-]), $\mathbf{K} = \mathbf{K}(\mathbf{x},\psi)$ is the hydraulic conductivity tensor ($[\mathrm{LT}^{-1}]$), $q_{\rm in} = q_{\rm in}(\mathbf{x},t)$, $q_{\rm in} \geq 0$, denotes the sources per unit volume ($[\mathrm{T}^{-1}]$), and $q_{\rm out} = q_{\rm out}(\mathbf{x},t)$, $q_{\rm out} \leq 0$, the sinks per unit volume ($[\mathrm{T}^{-1}]$).

The dependence of θ and $\mathbf{K}$ on ψ is given for example by the van Genuchten law (see [12]). First of all,

$$\begin{aligned}
\theta(\psi) &= \theta_{\rm r} + \frac{\theta_{\rm s}-\theta_{\rm r}}{(1+|\alpha\psi|^n)^m} \text{ if } \psi \leq 0\,, && (2.2)\\
\theta(\psi) &= \theta_{\rm s} \text{ if } \psi \geq 0\,,
\end{aligned}$$

where $\theta_{\rm r}$ is the residual water content, $\theta_{\rm s}$ is the saturated water content (i.e. porosity), $m = 1/n$, and $\alpha = \alpha(\mathbf{x})$ and $n = n(\mathbf{x})$ are two parameters. Next, one defines first the effective saturation $S_{\rm e}$ ([-]) by

$$S_{\rm e} = \frac{\theta-\theta_{\rm r}}{\theta_{\rm s}-\theta_{\rm r}} \tag{2.3}$$

and finally

$$\begin{aligned}
\mathbf{K}(\psi) &= \mathbf{K}_{\rm s} S_{\rm e}^{\frac{1}{2}}\left[1-\left(1-S_{\rm e}^{1/m}\right)^m\right]^2 \text{ if } \psi \leq 0\,, && (2.4)\\
\mathbf{K}(\psi) &= \mathbf{K}_{\rm s} \text{ if } \psi \geq 0\,,
\end{aligned}$$

where $\mathbf{K}_{\rm s}$ is the saturated hydraulic conductivity. Finally, the velocity field $\mathbf{v} = \mathbf{v}(\mathbf{x},t)$ ($[\mathrm{LT}^{-1}]$) is given by the Darcy law

$$\mathbf{v} = -\mathbf{K}(\psi)\nabla(\psi+z)\,. \tag{2.5}$$

2.2.2 Dupuit equation

Consider a layer $\Omega \in \mathbb{R}^3$ with bottom coordinate $z_{\rm b} = z_{\rm b}(x,y)$, top coordinate $z_{\rm t} = z_{\rm t}(x,y)$, and aperture $e = z_{\rm t} - z_{\rm b} = e(x,y)$, see Figure 2. The Dupuit approximation of the Richards equation (2.1a) in Ω consists in integrating the Richards equation over the aquifer aperture e under the assumption that the flow is only horizontal, cf. [2, 3]. We consider in addition the effect of water compressibility and a nonlinear discharge function. Let us denote by Ω' the horizontal plane

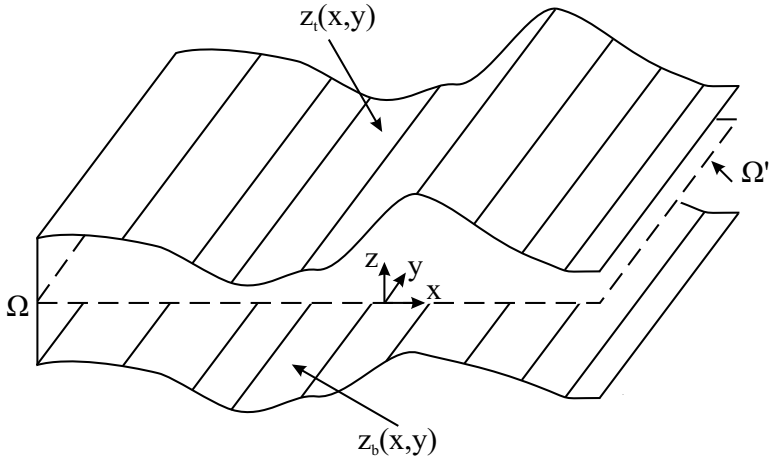

Figure 2: One layer $\Omega \in \mathbb{R}^3$ with its horizontal plane $\Omega' \in \mathbb{R}^2$

of Ω, cf. Figure 2, and by Γ'_{D} and Γ'_{N} the Dirichlet and Neumann boundaries of Ω', respectively. The problem then reads

$$\begin{aligned}
\frac{\partial \tilde{\theta}(h)}{\partial t} - \nabla \cdot \tilde{\mathbf{K}}(h) \nabla h + \tilde{Q}_d(h) &= \tilde{q}_{\mathrm{out}} + \tilde{q}_{\mathrm{in}} \quad \text{in } \Omega' \times (0,T)\,, && \text{(2.6a)}\\
h(\cdot,0) &= h_0 \quad \text{in } \Omega'\,, && \text{(2.6b)}\\
h &= h_D \quad \text{on } \Gamma'_{\mathrm{D}} \times (0,T)\,, && \text{(2.6c)}\\
-\tilde{\mathbf{K}}(h) \nabla h \cdot \mathbf{n} &= 0 \quad \text{on } \Gamma'_{\mathrm{N}} \times (0,T)\,, && \text{(2.6d)}
\end{aligned}$$

where h ([L]) is the piezometric head, $h = z + \psi$,

$$\frac{\partial \tilde{\theta}(h)}{\partial h} = \begin{cases} E_{\mathrm{l}} & \text{if } h \le z_{\mathrm{t}} \\ E_{\mathrm{s}} e & \text{if } h \ge z_{\mathrm{t}} \end{cases} \tag{2.7}$$

and

$$\tilde{\mathbf{K}}(h) = \begin{cases} \mathbf{K}_{\mathrm{s}}(h - z_{\mathrm{b}}) & \text{if } h \le z_{\mathrm{t}} \\ \mathbf{K}_{\mathrm{s}} e & \text{if } h \ge z_{\mathrm{t}} \end{cases} \tag{2.8}$$

and finally

$$\tilde{Q}_d(h) = \begin{cases} 0 & \text{if } h \le z_{\mathrm{t}} \\ \mathbf{K}_d(h - z_{\mathrm{t}}) & \text{if } h \ge z_{\mathrm{t}} \end{cases} . \tag{2.9}$$

The problem (2.6a)–(2.6d) is two-dimensional, all the variables and in particular the unknown piezometric head h are only functions of the horizontal coordinates x, y, and the gradient and divergence operators are also only two-dimensional. The storativity E_{l} ([-]) is related to the water content θ by $E_{\mathrm{l}} = \theta_{\mathrm{s}} - \theta_{\mathrm{r}}$. The specific storativity E_{s} ([L^{-1}]) is given by the water compressibility and is usually very small in comparison with E_{l}/e. The discharge $\tilde{Q}_d$ ([LT^{-1}]) depends on the hydraulic conductance $\mathbf{K}_d$ ([T^{-1}]). In analogy with the Darcy law (2.5), we define

$$\tilde{\mathbf{v}} := -\tilde{\mathbf{K}}(h) \nabla h\,. \tag{2.10}$$

Notice that $\tilde{\mathbf{v}}$ is a two-dimensional vector in Ω' with the units of [$\mathrm{L}^2\mathrm{T}^{-1}$]. The flux of $\tilde{\mathbf{v}}$ through a segment $\mathbf{b} \in \Omega'$, $\int_{\mathbf{b}} \mathbf{v}(\mathbf{x},t) \cdot \mathbf{n}_{\mathbf{b}}\, \mathrm{d}\gamma(\mathbf{x})$ ([$\mathrm{L}^3\mathrm{T}^{-1}$]), approximates the flux of groundwater over a vertical face in Ω, whose intersection with the horizontal plane Ω' is the segment $\mathbf{b}$.

The Dupuit equation can be used simultaneously in each layer. Since one is probably interested in simulating the entire 3D subsurface domain composed of individual layers (cf. the left part of Figure 1), an empirical condition is used in Talisman in order to connect the neighboring layers. One simply assumes that vertical exchange is given by a one-dimensional analogue of the Darcy law under the form

$$\mathbf{v}_{\mathrm{ver}} = \overline{\mathbf{K}}_{\mathrm{ver}}(h)\frac{h_{\mathrm{sup}} - h_{\mathrm{inf}}}{z_{\mathrm{sup}} - z_{\mathrm{inf}}}\,, \tag{2.11}$$

where h_{sup} and h_{inf} are respectively the piezometric heads in the superior and inferior layers and z_{sup} and z_{inf} are the vertical coordinates of the middles of the two layers. Finally, let $\mathbf{K}_{\mathrm{ver}}(h)$ ($[\mathrm{LT}^{-1}]$) be the vertical hydraulic conductivity given by

$$\mathbf{K}_{\mathrm{ver}}(h) = \begin{cases} \mathbf{K}_{\mathrm{ver,s}}(h - z_{\mathrm{b}}) & \text{if } h \leq z_{\mathrm{t}} \\ \mathbf{K}_{\mathrm{ver,s}}e & \text{if } h \geq z_{\mathrm{t}} \end{cases} \tag{2.12}$$

in each of the two layers, where $\mathbf{K}_{\mathrm{ver,s}}$ is the saturated vertical hydraulic conductivity in each of the two layers. Then we set $\overline{\mathbf{K}}_{\mathrm{ver}}$ as a suitable (harmonic rather than arithmetic) distance-weighted average of the two vertical hydraulic conductivities.

2.2.3 Hantush equation

Hantush equation is a further simplification of the Dupuit equation. Hantush approximation consists in supposing that the flow in the semi-permeable layers is essentially vertical (which is justified whenever the hydraulic conductivity of the semi-permeable layers is substantially lower than that of the surrounding aquifers). Then one may only consider the 2D multi-layer representation of the subsurface where the semi-permeable layers are not represented, as in the right part of Figure 1. In the aquifers, the Dupuit equation is considered, and the equation (2.11) is replaced by

$$\mathbf{v}_{\mathrm{ver}} = \mathbf{K}_{\mathrm{sp}}(h)\frac{h_{\mathrm{sup}} - h_{\mathrm{inf}}}{z_{\mathrm{sup}} - z_{\mathrm{inf}}}\,. \tag{2.13}$$

Here h_{sup} and h_{inf} are respectively the piezometric heads in the aquifer superior to and inferior to the concerned semi-permeable layer, z_{sup} is the bottom vertical coordinate of the superior aquifer, z_{inf} is the top vertical coordinate of the inferior aquifer, and $\mathbf{K}_{\mathrm{sp}}$ ($[\mathrm{LT}^{-1}]$) is the hydraulic conductivity of the semi-permeable layer, given by

$$\mathbf{K}_{\mathrm{sp}}(h) = \begin{cases} \mathbf{K}_{\mathrm{sp,s}}(h - z_{\mathrm{b}}) & \text{if } h \leq z_{\mathrm{t}} \\ \mathbf{K}_{\mathrm{sp,s}}e & \text{if } h \geq z_{\mathrm{t}} \end{cases}\,, \tag{2.14}$$

with $\mathbf{K}_{\mathrm{sp,s}}$ being the saturated vertical hydraulic conductivity in the semi-permeable layer ($e = z_{\mathrm{t}} - z_{\mathrm{b}}$ is this time the aperture of the semi-permeable layer).

2.2.4 Smoothing the Dupuit and Hantush functions

The equations (2.7), (2.8) and (2.9), as well as (2.12) and (2.14) prescribe nonlinear functions which are not differentiable. Since the Newton method (see Section 3.5 below) needs continuously differentiable functions, keeping the above-mentioned definition as such would lead to convergence problems in the numerical approximation using the Newton method. Moreover, the hydraulic conductivity definitions (2.8), (2.12), and (2.14) are only valid when $h > z_{\mathrm{b}} + m$ for some positive constant m, otherwise would lead to a negative hydraulic conductivity, whence its modification in the sense of the van Genuchten equation (2.4) is needed. Talisman thus actually uses the modifications given below.

Water content

Choosing a positive constant m, in [15] referred to as "minimal water thickness", we replace (2.7) by (θ corresponds to $\tilde{\theta}/e$):

$$\begin{aligned}
e &= z_\mathrm{t} - z_\mathrm{b}\,,\\
E_\mathrm{c} &= E_\mathrm{s}(z_\mathrm{t} - z_\mathrm{b})\,,\\
C_1 &= (E_\mathrm{l} - E_\mathrm{c})(z_\mathrm{t} - m) + (E_\mathrm{l} - E_\mathrm{c})/(2m)((z_\mathrm{t} - m)^2/2 - (z_\mathrm{t} - m)(z_\mathrm{t} + m))\,,\\
C_2 &= (E_\mathrm{l} - E_\mathrm{c})/(2m)((z_\mathrm{t} + m)^2/2) + C_1\,,\\
\alpha &= E_\mathrm{l} m^2\,,\\
\beta &= -z_\mathrm{b} - 2m\,;
\end{aligned}$$

$$\begin{aligned}
&\text{if } (h > z_\mathrm{t} + m)\\
&\qquad \theta = (E_\mathrm{c} h + C_2 - E_\mathrm{l} z_\mathrm{b})/e + \theta_\mathrm{s} - E_\mathrm{l}\,,\\
&\text{else if } (h > z_\mathrm{t} - m)\\
&\qquad \theta = (E_\mathrm{c} h - (E_\mathrm{l} - E_\mathrm{c})/(2m)(h^2/2 - (z_\mathrm{t} + m)h) + C_1 - E_\mathrm{l} z_\mathrm{b})/e + \theta_\mathrm{s} - E_\mathrm{l}\,,\\
&\text{else if } (h > z_\mathrm{b} + m)\\
&\qquad \theta = (E_\mathrm{l}(h - z_\mathrm{b}))/e + \theta_\mathrm{s} - E_\mathrm{l}\,,\\
&\text{else}\\
&\qquad \theta = (-\alpha/(h + \beta))/e + \theta_\mathrm{s} - E_\mathrm{l}\,.
\end{aligned}$$

Hydraulic conductivity

With the same "minimal water thickness" m, we replace (2.8) by ($\mathbf{K}$ corresponds to $\tilde{\mathbf{K}}/e$):

$$\begin{aligned}
e &= z_\mathrm{t} - z_\mathrm{b}\,,\\
c &= \mathbf{K}_\mathrm{s}\,,\\
d &= \mathbf{K}_\mathrm{s}(z_\mathrm{t} - m - z_\mathrm{b})\,,\\
a &= [(2m)\mathbf{K}_\mathrm{s} + 2(\mathbf{K}_\mathrm{s}(z_\mathrm{t} - m - z_\mathrm{b}) - \mathbf{K}_\mathrm{s} e)]/(2m)^3\,,\\
b &= [-\mathbf{K}_\mathrm{s} - 3a(2m)^2]/(4m)\,;
\end{aligned}$$

$$\begin{aligned}
&\text{if } (h \geq z_\mathrm{t} + m)\\
&\qquad \mathbf{K} = \mathbf{K}_\mathrm{s}\,,\\
&\text{else if } (h > z_\mathrm{t} - m)\\
&\qquad \mathbf{K} = (a(h - (z_\mathrm{t} - m))^3 + b(h - (z_\mathrm{t} - m))^2 + c(h - (z_\mathrm{t} - m)) + d)/e\,,\\
&\text{else if } (h > z_\mathrm{b} + m)\\
&\qquad \mathbf{K} = \mathbf{K}_\mathrm{s}(h - z_\mathrm{b})/e\,,\\
&\text{else if } (h > z_\mathrm{b})\\
&\qquad \mathbf{K} = \mathbf{K}_\mathrm{s}((h - z_\mathrm{b})^2/2/m + m/2)/e\,,\\
&\text{else}\\
&\qquad \mathbf{K} = \mathbf{K}_\mathrm{s} m/2/e\,.
\end{aligned}$$

Similar substitutions are applied in (2.12) and (2.14).

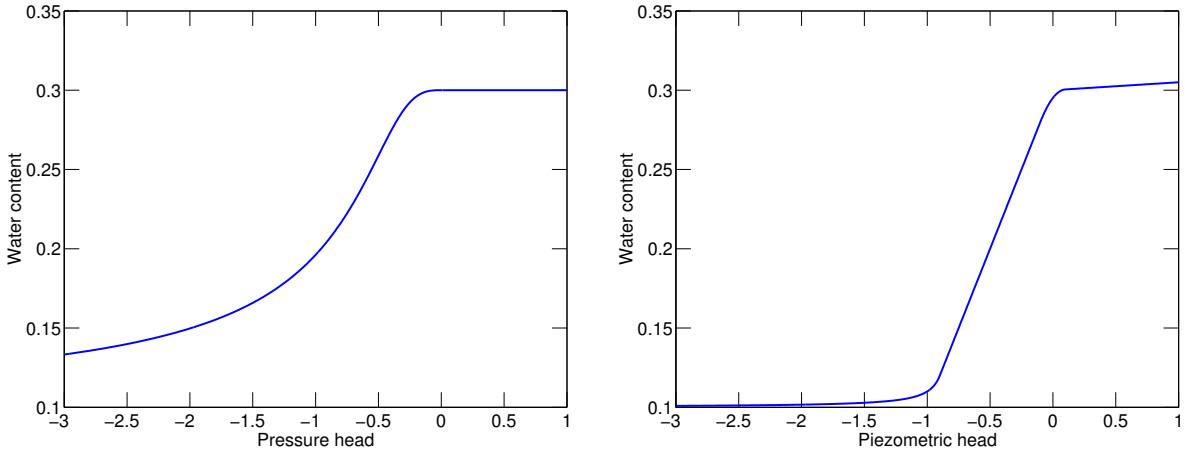

Figure 3: Comparison of water content curves ($\theta_\mathrm{r} = 0.1$, $\theta_\mathrm{s} = 0.3$, $E_\mathrm{l} = 0.2$, $E_\mathrm{s} = 0.005$) for the van Genuchten equation (2.2) (left, $\alpha = 2$, $n = 3$) and the smoothed Dupuit equation (2.7) (right, $z_\mathrm{t} = 0$, $z_\mathrm{b} = -1$, $m = 0.1$)

Discharge

Choosing a positive constant m, in [15] referred to as "minimal discharge height", we replace (2.9) by (Q_d corresponds to $\tilde{Q}_d/e$):

$$\mathbf{K} \;=\; \mathbf{K}_d/(z_\mathrm{t} - z_\mathrm{b})\,;$$

$$\begin{aligned}
&\text{if } (h \le z_\mathrm{t}) \\
&\qquad Q_d \;&=\; 0\,, \\
&\text{else if } (h < z_\mathrm{t} + m) \\
&\qquad Q_d \;&=\; 2\mathbf{K}/m(h - z_\mathrm{t})^2 - \mathbf{K}/m^2(h - z_\mathrm{t})^3\,, \\
&\text{else} \\
&\qquad Q_d \;&=\; \mathbf{K}(h - z_\mathrm{t})\,.
\end{aligned}$$

2.2.5 Comparison of the van Genuchten and smoothed Dupuit functions

We give comparisons of the van Genuchten and smoothed Dupuit water content and hydraulic conductivity functions in Figures 3 and 4.

2.3 Transport equation

In Talisman, a reactive miscible displacement with equilibrium adsorption of one contaminant in Ω is described by (see e.g. [1, 3, 8, 16])

$$\begin{aligned}
&\frac{\partial(\theta c)}{\partial t} + \rho_b \frac{\partial w(c)}{\partial t} - \nabla\cdot(\mathbf{S}\nabla c) + \nabla\cdot(c\mathbf{v}) \\
&\qquad +\lambda\left(\theta c + \rho_b w(c)\right) - q_\mathrm{out} c \;&=\; q_\mathrm{in} c_\mathrm{s} \quad \text{in } \Omega\times(0,T)\,, && \text{(2.15a)} \\
&\qquad\qquad c(\cdot,0) \;&=\; c_0 \quad \text{in } \Omega\,, && \text{(2.15b)} \\
&\qquad\qquad c \;&=\; g \quad \text{on } \partial\Omega\times(0,T)\,. && \text{(2.15c)}
\end{aligned}$$

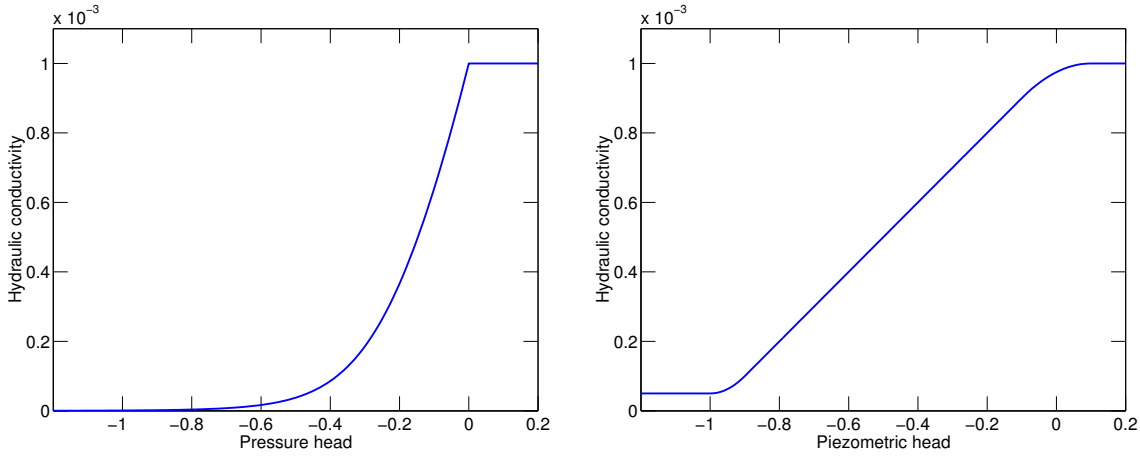

Figure 4: Comparison of hydraulic conductivity curves ($\mathbf{K}_\mathrm{s} = 10^{-3}$) for the van Genuchten equation (2.4) (left, $\theta_\mathrm{r} = 0.1$, $\theta_\mathrm{s} = 0.3$, $\alpha = 2$, $n = 3$) and the smoothed Dupuit equation (2.8) (right, $z_\mathrm{t} = 0$, $z_\mathrm{b} = -1$, $m = 0.1$)

In (2.15a)–(2.15c) $c = c(\mathbf{x}, t)$ is the unknown concentration of the dissolved contaminant ($[\mathrm{ML}^{-d}]$), $\theta = \theta(\mathbf{x}, t)$ is the water content given by (2.1a)–(2.1d) (see Section 3.4 below for the adjustments in the Dupuit or Hantush cases), $\rho_b = \rho_b(\mathbf{x})$ is the bulk density of the porous medium ($[\mathrm{ML}^{-d}]$), and $w : \mathbb{R} \to \mathbb{R}$ is the equilibrium adsorption function. We suppose that adsorption is sufficiently fast in comparison with the speed of the displacement of the contaminant so that the concentration of the dissolved contaminant c and the concentration ratio of the immobilized contaminant $w(c)$ ([-]) are in equilibrium. In particular, we shall consider, for $c \geq 0$, $w(c) = 0$ in the case of no adsorption, $w(c) = \mu_1 c$ in the case of the linear isotherm, $w(c) = \mu_1 c^{\mu_2}$ in the case of the Freundlich isotherm, and $w(c) = \mu_1\mu_2 c/(1 + \mu_1 c)$ in the case of the Langmuir isotherm. Here μ_1 ($[\mathrm{L}^d\mathrm{M}^{-1}]$) and μ_2 ([-]) are respectively the first and second adsorption parameters, which are supposed positive. Neumann or Robin boundary conditions can also be considered.

We suppose that the diffusion–dispersion tensor $\mathbf{S} = \mathbf{S}(\mathbf{x}, \mathbf{v})$ ($[\mathrm{L}^2\mathrm{T}^{-1}]$) is given by

$$\begin{aligned} \mathbf{S}_{ii} &= \alpha_T|\mathbf{v}| + (\alpha_L - \alpha_T)\frac{\mathbf{v}_i^2}{|\mathbf{v}|} + \sigma \qquad i = 1, \ldots, d\,, \\ \mathbf{S}_{ij} = \mathbf{S}_{ji} &= (\alpha_L - \alpha_T)\frac{\mathbf{v}_i\mathbf{v}_j}{|\mathbf{v}|} \qquad i, j = 1, \ldots, d\,, \end{aligned}$$

where $\mathbf{v}_i$ are the components of the Darcy velocity vector $\mathbf{v}$ (2.5) and $|\mathbf{v}|$ is its length, $\alpha_L = \alpha_L(\mathbf{x})$ is the longitudinal dispersivity ([L]), $\alpha_T = \alpha_T(\mathbf{x})$ is the transverse dispersivity ([L]), and finally $\sigma = \sigma(\mathbf{x})$ is the molecular diffusion coefficient ($[\mathrm{L}^2\mathrm{T}^{-1}]$). We consider first-order irreversible reactions such as radioactive decay, hydrolysis, and some forms of biodegradation, where λ is the reaction rate constant ($[\mathrm{T}^{-1}]$). Finally, in the case of a source ($q_\mathrm{in} \geq 0$), we have to specify the concentration of the entering dissolved contaminant c_s. In contrast, the concentration of the leaving dissolved contaminant due to the sinks ($q_\mathrm{out} \leq 0$) is given by the unknown concentration c.

3 Numerical schemes

We describe here the numerical schemes used in Talisman.

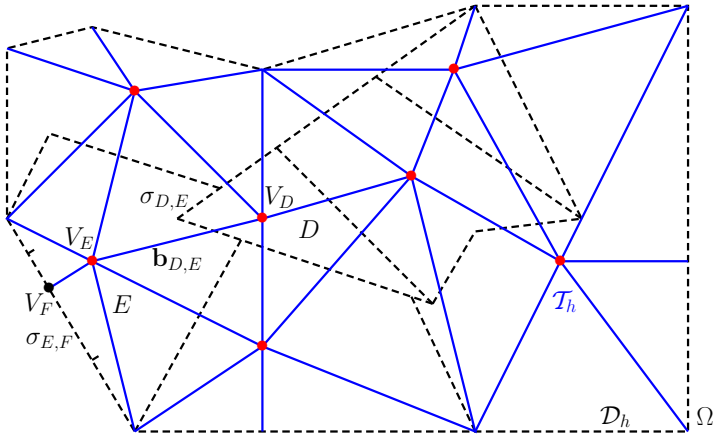

Figure 5: Primal nonmatching grid $\mathcal{D}_h$ (dashed) and dual triangular grid $\mathcal{T}_h$ (solid)

3.1 Space and time discretizations

We suppose a generally nonconstant time step for the time discretization. We split up the time interval $(0,T)$ such that $0 = t_0 < \ldots < t_n < \ldots < t_N = T$ and define $\triangle t_n := t_n - t_{n-1}$, $n \in \{1, 2, \ldots, N\}$. We next describe the space discretization.

As a *primal grid* of Ω, we understand a partition $\mathcal{D}_h$ of Ω into closed polygons such that $\overline{\Omega} = \bigcup_{D\in\mathcal{D}_h} D$ and such that the intersection of interiors of two different polygons is empty. We in particular admit nonmatching grids, i.e. the case where there exist two different polygons $D, E \in \mathcal{D}_h$ such that their intersection is not an empty set but it is not a common vertex, edge, or side (edge if $d = 2$, face if $d = 3$) of D and E. An example of an admissible primal grid is given in Figure 5 by the dashed line. We suppose that there exists a family of points $\mathcal{P}_h$ such that there is one point V_D in the interior of D associated with each $D \in \mathcal{D}_h$.

A *dual grid* of Ω is a partition $\mathcal{T}_h$ of Ω into closed simplices which satisfies the following properties: (i) The set of points $\mathcal{P}_h$ is contained in the set of vertices of $\mathcal{T}_h$, denoted by $\mathcal{V}_h$; (ii) The vertices from $\mathcal{V}_h \setminus \mathcal{P}_h$ lie on the boundary of Ω; (iii) $\mathcal{T}_h$ is conforming, i.e. the intersection of two different simplices is either an empty set or their common vertex, edge, or face; (iv) $\overline{\Omega} = \bigcup_{K\in\mathcal{T}_h} K$. This definition is not unique: we have a choice in connecting the different points $V_D \in \mathcal{P}_h$ and also a choice in the definition of the vertices on the boundary. The general intention is to find a triangulation such that the transmissibilities $\mathbb{S}^n_{D,E}$ defined below by (3.2) were non-negative, since this implies the discrete maximum principle. An example of a dual grid to a primal nonmatching grid is given in Figure 5 by the solid line.

In order to simplify the notation, we define still a *fictitious boundary grid* $\mathcal{D}_h^{\mathrm{ext}}$. We associate a fictitious control volume D with each vertex $V \in \mathcal{V}_h$ lying on the boundary $\partial\Omega$. We define D in such way that $D \cap \Omega = \emptyset$, $D \cap \overline{\Omega} \subset \partial\Omega$, and $V \in D \cap \overline{\Omega}$. We finally require that the boundaries of D, $D \in \mathcal{D}_h^{\mathrm{ext}}$, halve the segments of $\partial\Omega$ between the boundary vertices, so that $\cup_{D\in\mathcal{D}_h^{\mathrm{ext}}} \{D \cap \overline{\Omega}\} = \partial\Omega$. We shall use the notation V_D for the vertex associated with $D \in \mathcal{D}_h^{\mathrm{ext}}$, as for the vertices from $\mathcal{P}_h$ and control volumes from $\mathcal{D}_h$.

We finally denote by $\mathcal{N}(D)$ the set of all neighbors of a control volume $D \in \mathcal{D}_h$, i.e. the set of $E \in \mathcal{D}_h \cup \mathcal{D}_h^{\mathrm{ext}}$ such that $D \cap E$ has a positive $(d-1)$-dimensional measure. In particular, using the above definition of the set $\mathcal{D}_h^{\mathrm{ext}}$, we can easily write the integral over ∂D as $\sum_{E\in\mathcal{N}(D)} \int_{\partial D\cap\partial E} \mathrm{d}\gamma(\mathbf{x})$. Similarly, for a vertex $V_D \in \mathcal{P}_h$, we denote by $\mathcal{M}(V_D)$ the set of all vertices $V_E \in \mathcal{V}_h$ such that there exists an edge between V_D and V_E. In Talisman, the grids actually used are much simpler and we refer to Figure 6 for an example.

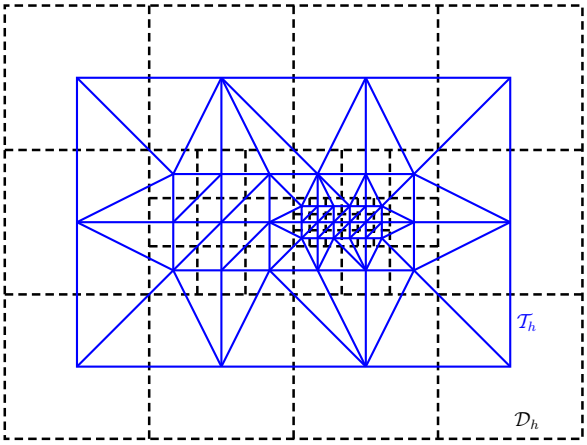

Figure 6: Primal (dashed) and dual (solid) grids used in Talisman

3.2 Combined finite volume–finite element scheme for transport

The combined scheme is obtained by the discretization of the diffusion term of (2.15a) by means of the piecewise linear conforming finite element method on $\mathcal{T}_h$, the discretization of the other terms of (2.15a) by means of the cell-centered finite volume method on $\mathcal{D}_h$, and using a finite difference time stepping.

Definition 3.1. (Combined finite volume–finite element scheme) *The fully implicit combined finite volume–finite element scheme for the problem (2.15a)–(2.15c) reads: find the values c_D^n, $D \in \mathcal{D}_h$, $n \in \{0, 1, \ldots, N\}$, such that*

$$c_D^0 = \frac{1}{|D|} \int_D c_0(\mathbf{x})\, \mathrm{d}\mathbf{x} \qquad D \in \mathcal{D}_h\,, \tag{3.1a}$$

$$c_D^n = g(V_D, t_n) \qquad D \in \mathcal{D}_h^{\mathrm{ext}}\,,\ n \in \{1, 2, \ldots, N\}\,, \tag{3.1b}$$

$$\begin{aligned} &\frac{\theta_D^n c_D^n - \theta_D^{n-1} c_D^{n-1}}{\triangle t_n} |D| + (\rho_b)_D \frac{w(c_D^n) - w(c_D^{n-1})}{\triangle t_n}\, |D| - \sum_{V_E \in \mathcal{M}(V_D)} \mathbb{S}_{D,E}^n (c_E^n - c_D^n) \\ &+ \sum_{E \in \mathcal{N}(D)} \mathbf{v}_{D,E}^n\, \overline{c_{D,E}^n} + \lambda[\theta_D^n c_D^n + (\rho_b)_D w(c_D^n)]|D| - (q_{\mathrm{out}})_D^n c_D^n |D| = (q_{\mathrm{in}} c_s)_D^n |D| \\ &\qquad D \in \mathcal{D}_h\,,\ n \in \{1, 2, \ldots, N\}\,. \end{aligned} \tag{3.1c}$$

In the above definition we have used

$$\begin{aligned} \theta_D^n &:= \frac{1}{|D|} \int_D \theta(\mathbf{x}, t_n) \qquad D \in \mathcal{D}_h\,,\ n \in \{0, 1, \ldots, N\}\,, \\ (\rho_b)_D &:= \frac{1}{|D|} \int_D \rho_b(\mathbf{x}) \qquad D \in \mathcal{D}_h\,, \\ (q_{\mathrm{out}})_D^n &:= \frac{1}{\triangle t_n |D|} \int_{t_{n-1}}^{t_n} \int_D q_{\mathrm{out}}(\mathbf{x}, t)\, \mathrm{d}\mathbf{x}\, \mathrm{d}t \qquad D \in \mathcal{D}_h\,,\ n \in \{1, 2, \ldots, N\}\,, \\ (q_{\mathrm{in}} c_s)_D^n &:= \frac{1}{\triangle t_n |D|} \int_{t_{n-1}}^{t_n} \int_D q_{\mathrm{in}}(\mathbf{x}, t) c_s(\mathbf{x}, t)\, \mathrm{d}\mathbf{x}\, \mathrm{d}t \qquad D \in \mathcal{D}_h\,,\ n \in \{1, 2, \ldots, N\} \end{aligned}$$

and we have denoted the flux of $\mathbf{v}$ between $D \in \mathcal{D}_h$ and $E \in \mathcal{N}(D)$ for $n \in \{1, 2, \ldots, N\}$ by

$$\mathbf{v}_{D,E}^n := \frac{1}{\triangle t_n} \int_{t_{n-1}}^{t_n} \int_{\partial D \cap \partial E} \mathbf{v}(\mathbf{x}, t) \cdot \mathbf{n}_{D,E} \, \mathrm{d}\gamma(\mathbf{x}) \, \mathrm{d}t \,,$$

where $\mathbf{n}_{D,E}$ is the unit normal vector of the side $\partial D \cap \partial E$ between D and E, outward to D. For the notational convenience, we define $\mathbf{v}_{D,E}^n$ by 0 if $E \notin \mathcal{N}(D)$. We suppose that the functions g and θ are sufficiently smooth in order to define c_D^n, $D \in \mathcal{D}_h^{\mathrm{ext}}$, and θ_D^n. We first define

$$\widetilde{\mathbf{S}}^n(\mathbf{x}) := \frac{1}{\triangle t_n} \int_{t_{n-1}}^{t_n} \mathbf{S}(\mathbf{x}, t) \, \mathrm{d}t \qquad \mathbf{x} \in \Omega \,,\, n \in \{1, 2, \ldots, N\} \,.$$

The transmissibility between V_D and V_E, $D \in \mathcal{D}_h$, $E \in \mathcal{D}_h \cup \mathcal{D}_h^{\mathrm{ext}}$, is then given by

$$\mathbb{S}_{D,E}^n := -\int_\Omega \mathbf{S}^n \nabla \varphi_E \cdot \nabla \varphi_D \, \mathrm{d}\mathbf{x} \qquad n \in \{1, 2, \ldots, N\} \,, \tag{3.2}$$

where we have two choices of the definition of $\mathbf{S}^n$. We can either use directly $\mathbf{S}^n = \widetilde{\mathbf{S}}^n$, or define a piecewise constant tensor

$$\mathbf{S}^n(\mathbf{y}) = \left(\frac{1}{|K|} \int_K [\widetilde{\mathbf{S}}^n(\mathbf{x})]^{-1} \, \mathrm{d}\mathbf{x} \right)^{-1} \qquad \mathbf{y} \in K \,,\, K \in \mathcal{T}_h \,,\, n \in \{1, 2, \ldots, N\} \,.$$

These two choices correspond, respectively, to the arithmetic or harmonic average of the diffusion–dispersion tensor.

Finally, we define the value $\overline{c_{D,E}^n}$ for $D \in \mathcal{D}_h$, $E \in \mathcal{N}(D)$, and $n \in \{1, 2, \ldots, N\}$ as follows:

$$\overline{c_{D,E}^n} := \begin{cases} c_D^n + \alpha_{D,E}^n (c_E^n - c_D^n) & \text{if } \mathbf{v}_{D,E}^n \geq 0 \\ c_E^n + \alpha_{D,E}^n (c_D^n - c_E^n) & \text{if } \mathbf{v}_{D,E}^n < 0 \end{cases} .$$

Here $\alpha_{D,E}^n$ is the coefficient of the amount of upstream weighting which is defined by

$$\alpha_{D,E}^n := \frac{\max\left\{\min\left\{\mathbb{S}_{D,E}^n, \frac{1}{2}|\mathbf{v}_{D,E}^n|\right\}, 0\right\}}{|\mathbf{v}_{D,E}^n|} \,, \quad \mathbf{v}_{D,E}^n \neq 0 \,. \tag{3.3}$$

We set $\alpha_{D,E}^n := 0$ if $\mathbf{v}_{D,E}^n$=0. We remark that usually, there can be nonzero convective and diffusive fluxes between D and E only if D and E neighbors. This is however not the case with the scheme (3.1a)–(3.1c): there can be nonzero convective flux between D and E only if D and E neighbors, but there can be nonzero diffusive flux between D and E even if D and E are not neighbors (because the transmissibility between D and E is given by the grid $\mathcal{T}_h$). However, as it is proved in [13, Theorem 1.9.4], the local Péclet upstream weighting still guarantees, adding minimal numerical diffusion, the stability of the scheme.

Other important properties of the scheme, like local mass conservation, stability, and convergence are proved in [13, Appendix 1.9], [5], and some analogies can also be found in [6].

3.3 Finite volume scheme and the flow case

On rectangular grids, or when the diffusion–dispersion tensor $\mathbf{S}$ reduces to a scalar function, it is not necessary to introduce the dual grid. Then a pure finite volume scheme may be used instead of

the combined one. This modification consists in replacing the term $-\sum_{V_E\in\mathcal{M}(V_D)}\mathbb{S}^n_{D,E}(c^n_E-c^n_D)$ in 3.1c by $-\sum_{V_E\in\mathcal{N}(D)}\mathbb{S}^n_{D,E}(c^n_E-c^n_D)$ and redefining $\mathbb{S}^n_{D,E}$ given by (3.2) as

$$\mathbb{S}^n_{D,E}:=\mathbf{S}^n\frac{|\sigma_{D,E}|}{|\mathbf{b}_{D,E}|}. \tag{3.4}$$

We refer for details to e.g. [4]. The flow equation (2.1a)–(2.1d) is in terms of discretization similar to the transport one (2.15a)–(2.15c) and the finite volume or combined finite volume–finite element schemes can likewise be used for its approximation.

3.4 Adjustments in the Dupuit/Hantush cases

In the Dupuit/Hantush cases, one supposes that the flow is only horizontal, see Section 2.2.2. In this case, similar approximations are to be made for the contaminant transport problem (2.15a)–(2.15c). We namely suppose that the concentration c does not vary with z and that the diffusion and convection are only two-dimensional in the horizontal plane Ω' of Ω. By formally integrating the three-dimensional convection–reaction–diffusion equation in Ω over e and adding the discharge, we replace the functions θ, $q_{\rm in}$, and $q_{\rm out}$ defined in Ω by the functions $\tilde\theta$, $\tilde q_{\rm in}$, and $\tilde q_{\rm out}-\tilde Q_d(h)$ defined in Ω'. We finally use $\tilde{\mathbf{v}}$ instead of $\mathbf{v}$ in the convection term and in the definition of the diffusion–dispersion tensor $\mathbf{S}$ and consider the gradient and divergence operators only in Ω'. Notice that we have to replace the molecular diffusion coefficient σ by $\tilde\sigma=\sigma e$. Hence the final transport problem is, as the flow problem, two-dimensional in the plane Ω', with the three-dimensional units (namely, the concentration is measured in $[\mathrm{ML}^{-3}]$).

With the assumptions of the previous paragraph, the transport scheme is constructed as follows. We consider a (nonmatching locally refined) square grid $\mathcal{D}_h$ of Ω' and its dual triangular grid $\mathcal{T}_h$, as that in Figures 5 or 6. We associate with each $D\in\mathcal{D}_h$ an aperture e_D, given for instance as the mean of e over D. We seek the values c^n_D, $D\in\mathcal{D}_h$, $n\in\{1,2,\dots,N\}$, such that

$$\begin{aligned}&\frac{\tilde\theta^n_D c^n_D-\tilde\theta^{n-1}_D c^{n-1}_D}{\triangle t_n}|D|+(\rho_b)_D\frac{w(c^n_D)-w(c^{n-1}_D)}{\triangle t_n}\,|D|e_D-\sum_{V_E\in\mathcal{M}(V_D)}\tilde{\mathbb{S}}^n_{D,E}(c^n_E-c^n_D)\\
&+\sum_{E\in\mathcal{N}(D)}\tilde{\mathbf{v}}^n_{D,E}\,\overline{c^n_{D,E}}+\lambda[\tilde\theta^n_D c^n_D+(\rho_b)_D w(c^n_D)e_D]|D|-[\tilde q_{\rm out}-\tilde Q_d(h)]^n_D c^n_D|D|=(\tilde q_{\rm in}c_{\rm s})^n_D|D|\\
&\qquad D\in\mathcal{D}_h\,,\ n\in\{1,2,\dots,N\}\end{aligned} \tag{3.5}$$

with appropriately prescribed initial and boundary conditions. Here $\tilde\theta^n_D$, $D\in\mathcal{D}_h$, $n\in\{0,1,\dots,N\}$, are the approximations of $\tilde\theta$ from (2.6a), given by a flow numerical scheme. In a similar manner, $\tilde{\mathbf{v}}^n_{D,E}$ are the approximations of the flux of $\tilde{\mathbf{v}}$ given by (2.10) through the interface between the control volumes $D\in\mathcal{D}_h$, $E\in\mathcal{N}(D)$ at time t_n. Note that from (2.6a) and using either the finite volume or combined finite volume–finite element scheme, which are both locally conservative, one has $\tilde{\mathbf{v}}^n_{D,E}=-\tilde{\mathbf{v}}^n_{E,D}$. We define $(\rho_b)_D$ e.g. as the mean of the bulk density ρ_b over the cube $D\times e_D$. The transmissibilities $\tilde{\mathbb{S}}^n_{D,E}$ are defined by (3.2), while employing $\tilde{\mathbf{v}}$ and $\tilde\sigma$ in the definition of the diffusion–dispersion tensor $\mathbf{S}$ instead of $\mathbf{v}$ and σ. Note finally that again for non-negative transmissibilities, the scheme verifies the discrete maximum principle, which is in particular the consequence of $\nabla\cdot\tilde{\mathbf{v}}=\tilde q_{\rm out}+\tilde q_{\rm in}-\tilde Q_d(h)-\partial\tilde\theta/\partial t$ following from (2.6a) and (2.10).

3.5 Newton method for linearization

The Newton method, see e.g. [9], is used for the solution of the system of nonlinear algebraic equations arising from (3.1a)–(3.1c) or (3.5). In particular, using the smoothing of the Dupuit and Hantush functions discussed in Section 2.2.4 is important in this respect.

3.6 Bi-CGStab method for the solution of sparse linear systems

The Bi-CGStab iterative method, see [11] or [10], is used for solution of the large sparse linear systems arising in the Newton method.

4 A posteriori error estimates

Two types of a posteriori error estimators are at disposition in Talisman. The first one is of the Zienkiewicz–Zhu type (cf. [17]) and is asymptotically exact (when the mesh size tends to zero, the estimate on the error given by this estimator tends to the true error in the approximation), works for all the models treated by Talisman, but does not give a guaranteed upper bound on the error. The second one is rigorously-based, gives a guaranteed upper bound on the error in the approximation, but is only applicable on the linear form of (3.1a)–(3.1c) or of (3.5).

4.1 Gradient estimates

Let $c_{h,\tau}$ be a piecewise constant function in time and space (on the mesh $\mathcal{D}_h$), given by the solution values c_D^n, $D \in \mathcal{D}_h$, $n \in \{0, 1, \ldots, N\}$ of (3.1a)–(3.1c) or of (3.5). Let next $\tilde{c}_{h,\tau}$ be a piecewise linear in time and space function given by $\sum_{D\in\mathcal{D}_h} c_D^n \varphi_D$. Let finally c be the exact solution of (2.15a)–(2.15c). The triangle inequality implies

$$\left(\int_0^T \int_\Omega (c - c_{h,\tau})^2 \,\mathrm{d}\mathbf{x}\,\mathrm{d}t\right)^{\frac{1}{2}} \leq \left(\int_0^T \int_\Omega (c - \tilde{c}_{h,\tau})^2 \,\mathrm{d}\mathbf{x}\,\mathrm{d}t\right)^{\frac{1}{2}} + \left(\int_0^T \int_\Omega (\tilde{c}_{h,\tau} - c_{h,\tau})^2 \,\mathrm{d}\mathbf{x}\,\mathrm{d}t\right)^{\frac{1}{2}}.$$

Since the approximate solution $\tilde{c}_{h,\tau}$ is piecewise linear, one may expect that it will converge faster to the solution c than $c_{h,\tau}$, whence the error will be in the limit case only given by the second term of the above expression. One may thus use this term as an asymptotically exact a posteriori error estimator.

4.2 Residual estimates

Residual estimates for the linear form of the scheme (3.1a)–(3.1c) are rigorously derived in [7].

5 Talisman execution diagram

We finally give in this section Talisman execution diagram. We remark that time or space adaptivity being chosen is sufficient so that one calculates both time and space a posteriori error estimates, since we need them in the a posteriori estimate of the error. We finally notice that for permanent models, the specified number of periods and number of steps per period is stored and temporarily replaced by one period of unit length and one time step in this period, so that the below diagrams were applicable.

5.1 General execution diagram

- choose parameter groups that will be necessary (`ParamGeom` and `ParamFlow` for the flow model, `ParamTrans` in addition for the transport model, `ParamApost` in the space adaptive mode)
- mark the given mesh (will be called fixed, whereas the adaptive will be called actual)

• set coordinates, number mesh cells, set up contact list, set minimal surface, create triangle mesh (if necessary)

• set correct flow sources units (originally given in $[L^3T^{-1}]$, we need them in $[T^{-1}]$)

• associate zeros to parameters which will be calculated during the execution (not given by the user): recharge and sources for flow, concentrations at sources and concentration fluxes in addition for transport

• verify that geometrical data are correct (2D multi-layer/3D models), that the data are in the user-specified intervals and that there are no isolated cells (not connected to the others) and no pseudo-isolated cells (that would not be a node of any triangle) if the FV–FE scheme is chosen

• open files for writing (`horloge.txt` for execution information, `MaillesSuspectes.txt` for mesh cells with dubious results (no convergence), `piezo.txt` for flow results and binary `mesh.out` for storing the original mesh before flow calculation was launched if flow, `conc.txt` for transport results if transport)

• create matrix and vectors

• set up initial conditions (for transient cases, copy the unknown quantity values given by user (piezometric head, concentration) to `-prev` unknowns)

• for transport coupled with permanent flow, set up flow conditions here (as they do not change in time, just once is enough); if there is space adaptivity, these flow conditions will be easily interpolated and extrapolated to the given mesh, since one does it in a piecewise constant manner

for all periods

  for all time steps

    • execute the time adaptivity loop

    • actualize execution information window, visualize, write results

    • if transient and space adaptivity, derefine cells without error and update coordinates, number mesh cells, set up contact list, set minimal surface, create triangle mesh, change matrix and vectors size

  end

end

• if adaptive calculation, decide whether the prescribed maximal error was attained

• close files for writing

• change back sources units

• unmark the given mesh

5.2 Time adaptivity execution diagram

• if reached the time level given by the time period and time step, go back to the main execution

• otherwise set up the conditions (recharge, sources, and Dirichlet boundary conditions for flow and Dirichlet boundary conditions, concentrations at sources, and concentration fluxes for transport) on the given time level and mesh

• for transport coupled with transient flow, set flow conditions here (for permanent flow it was already done before)

• execute the space adaptivity loop (get space error if space adaptivity)

• if there is time or space adaptivity, evaluate the norm of the approximate solution on the given time step; if transient case in addition, compute time a posteriori error estimate and set up time refinement criterion

• if time adaptivity, the error is too large, and maximal refinement not yet reached, refine time step and go back to the beginning of the time adaptivity loop

• otherwise we accept the computed result: store it as a previous value (`-prev` unknowns), increase the full error (space plus time one) and the norm of the approximate solution by the just finished time step, increase time level, and go back to the beginning of the time adaptivity loop

5.3 Space adaptivity execution diagram

• if transport, execute Newton loop for flow to get flow field and then compute the diffusion–dispersion tensor

• execute Newton loop

• if there is time or space adaptivity, compute space a posteriori error estimate and the norm of the approximate solution on the given time step and set up space refinement criterion

• if space adaptivity, the error is too large, and maximal refinement not yet reached, refine cells with error and update coordinates, number mesh cells, set up contact list, set minimal surface, create triangle mesh, change matrix and vectors size and go back to the beginning of the space adaptivity loop

• otherwise go back to the time adaptivity loop

5.4 Newton method execution diagram

• assemble matrix

• solve the linear system

• if linear case (transport without adsorption), go back to the space adaptivity loop

• otherwise evaluate error in the linearization; if too big and maximal number of iterations not yet reached, go back to the beginning of the Newton loop

References

[1] J. W. Barrett and P. Knabner, *Finite element approximation of the transport of reactive solutes in porous media. I. Error estimates for nonequilibrium adsorption processes*, SIAM J. Numer. Anal., 34 (1997), pp. 201–227.

[2] J. Bear, *Dynamics of Fluids in Porous Media*, American Elsevier, New York, 1972.

[3] J. Bear and A. Verruijt, *Modelling Groundwater Flow and Pollution*, vol. 2 of Theory and Applications of Transport in Porous Media, Kluwer Academic Publisher, Dordrecht, Holland, 1987.

[4] R. Eymard, T. Gallouët, and R. Herbin, *Finite volume methods*, in Handbook of Numerical Analysis, Vol. VII, North-Holland, Amsterdam, 2000, pp. 713–1020.

[5] R. Eymard, D. Hilhorst, and M. Vohralík, *A combined finite volume–finite element scheme for the discretization of strongly nonlinear convection–diffusion–reaction problems on nonmatching grids*, Submitted, (2006).

[6] ——, *A combined finite volume–nonconforming/mixed-hybrid finite element scheme for degenerate parabolic problems*, Numer. Math., 105 (2006), pp. 73–131.

[7] D. Hilhorst and M. Vohralík, *A posteriori error estimates for combined finite volume–finite element discretizations of reactive transport equations on nonmatching grids*, In preparation, (2006).

[8] I. Javandel, C. Doughty, and C. Tsang, *Groundwater Transport: Handbook of Mathematical Models*, vol. 10, American Geophysical Union Water Resources Monograph Series, New York, 1984.

[9] A. Quarteroni, R. Sacco, and F. Saleri, *Numerical mathematics*, vol. 37 of Texts in Applied Mathematics, Springer-Verlag, New York, 2000.

[10] A. Quarteroni and A. Valli, *Numerical approximation of partial differential equations*, vol. 23 of Springer Series in Computational Mathematics, Springer-Verlag, Berlin, 1994.

[11] H. A. van der Vorst, *Bi-CGSTAB: a fast and smoothly converging variant of Bi-CG for the solution of nonsymmetric linear systems*, SIAM J. Sci. Statist. Comput., 13 (1992), pp. 631–644.

[12] M. van Genuchten, *A closed form for predicting the hydraulic conductivity of unsaturated soils*, Soil Sci. Soc. Amer. J., 44 (1980), pp. 892–898.

[13] M. Vohralík, *Méthodes numériques pour des équations elliptiques et paraboliques non linéaires. Application à des problèmes d'écoulement en milieux poreux et fracturés*, thèse de doctorat, Université de Paris-Sud & Université Technique Tchèque à Prague, décembre 2004.

[14] M. Vohralík and L. Inovecký, *Talisman, a finite volume–finite element tool for numerical simulation of subsurface flow and contaminant transport with a posteriori error control and adaptive mesh refinement. Developer's manual*, HydroExpert, 53 rue Charles Frérot, 94 250 Gentilly, France, `www.hydroexpert.com`, (2007).

[15] M. Vohralík and N. Ramarosy, *Talisman, a finite volume–finite element tool for numerical simulation of subsurface flow and contaminant transport with a posteriori error control and adaptive mesh refinement. Presentation and User guide*, HydroExpert, 53 rue Charles Frérot, 94 250 Gentilly, France, `www.hydroexpert.com`, (2007).

[16] C. Zheng and G. Bennett, *Applied Contaminant Transport Modeling*, Van Nostrand Reinhold, New York, 1995.

[17] O. C. Zienkiewicz and J. Z. Zhu, *A simple error estimator and adaptive procedure for practical engineering analysis*, Internat. J. Numer. Methods Engrg., 24 (1987), pp. 337–357.